



HAL
open science

Sedimentologic Analysis of Cores Recovered from the RV Marion Dufresne

Viviane Bout-roumazeilles, Alain Trentesaux

► **To cite this version:**

Viviane Bout-roumazeilles, Alain Trentesaux. Sedimentologic Analysis of Cores Recovered from the RV Marion Dufresne. U.S. Geological Survey Professional Paper, 2007. <hal-03299741>

HAL Id: hal-03299741

<https://hal.science/hal-03299741v1>

Submitted on 26 Jul 2021

HAL is a multi-disciplinary open access archive for the deposit and dissemination of scientific research documents, whether they are published or not. The documents may come from teaching and research institutions in France or abroad, or from public or private research centers.

L'archive ouverte pluridisciplinaire **HAL**, est destinée au dépôt et à la diffusion de documents scientifiques de niveau recherche, publiés ou non, émanant des établissements d'enseignement et de recherche français ou étrangers, des laboratoires publics ou privés.



HAL Authorization

Sedimentologic Analysis of Cores Recovered from the RV *Marion Dufresne* Cruise in the Gulf of Mexico, 2–18 July 2002

Viviane Bout-Roumazielles¹ and Alain Trentesaux¹

¹. UMR8110 CNRS Processus et Bilans des Domaines Sédimentaires PBDS University of Lille I, 59655 Villeneuve d'Ascq, France.

Sedimentologic analysis of cores recovered from the RV *Marion Dufresne* cruise in the Gulf of Mexico, 2–18 July 2002; chapter 5 in Winters, W.J., Lorenson, T.D., and Paull, C.K., eds., 2007, Initial report of the IMAGES VIII/PAGE 127 gas hydrate and paleoclimate cruise on the RV *Marion Dufresne* in the Gulf of Mexico, 2–18 July 2002: U.S. Geological Survey Open-File Report 2004–1358.

Introduction

The Gulf of Mexico is a small ocean basin surrounded by land masses. It is connected to the Atlantic Ocean through the Florida Strait to the east and to the Caribbean Sea through the Yucatan channel (fig. 1). Numerous topics have been studied in the Gulf of Mexico, including sediment transport (Coleman and others, 1991), mineralogy (Griffin, 1962), grain size (Mazzullo and Bates, 1985; Mazzullo, 1986), and more recently, sea-floor sediment distribution (Balsam and Beeson, 2003). These studies confirm the major influence of sediment supplied by the Mississippi River on the composition of the Gulf of Mexico sediments. In fact, sediments transported by the Mississippi River spread out over the Texas, Louisiana, and Mississippi shelves, and reach the Mississippi deep-sea fan and the Sigsbee abyssal plain (Bouma and others, 1985; Davies and Moore, 1970).

The Gulf of Mexico is divided into two morphological and sedimentological provinces (fig. 1), separated by the De Soto Canyon to the northeast and the Campeche Canyon to the southwest (Burk and Drake, 1974; Nairn and Stehli, 1975):

- a northwestern terrigenous province—the Mississippi Delta, the abyssal plain, and the northern, western, and southern continental shelves; and
- a southeastern calcareous province—the Campeche bank and the Florida bank.

Much of the sea floor is dominated by salt-tectonic basin structures, high sedimentation rates, and complex stratigraphy with common sea-floor failures (Cooper and

Hart, 2002). Natural oil and gas seeps are abundant, usually associated with fault conduits resulting in numerous hydrocarbon vents, often capped by gas hydrate when the seeps are within the hydrate stability zone. While gas hydrate is relatively common at the sea floor (Sassen and others, 1999), the lack of geophysical indicators on seismic records leaves the existence of deeper gas hydrates unresolved. Thus, it is unknown if there are significant gas hydrate accumulations in reservoir sediments away from structural conduits inferred to underlie the seafloor mounds. The geologic setting and its influence on site selection for this cruise are further discussed by Lorenson and others (this volume, chapter 2).

Methods

Seventeen giant Calypso piston cores, up to 38 meters to 10 m long, and four gravity cores up to 9 m long (Winters and others, this volume, chapter 3) were recovered along chirp seismic-reflection transects in widely different geologic environments (fig. 2; Appendix A) in water depths ranging from 580 to 2,260 m. For each core, a corresponding trackline map and 3.5 kilohertz (kHz) seismic profile are presented in Appendix D. Note that the arrows labeled “Carotte” in the figures in Appendix D represent piston-core locations.

Core Handling and Sampling Procedures

As soon as the core arrived onboard, sediment from the core cutter and catcher was bagged. The core liner was then pulled out of the barrel and the ends were capped. A meter tape was used to measure the length of the core and to mark precisely each 1.5-m-long section. Using the predefined orientation line as a guide, the starboard side of each core was identified as the “working” half and the port side as the “archive” half. Each section was identified with the core number (Arabic number), section number (Roman numeral), and the depth of the section top and bottom. The sections were then cut with a core cutter, capped, and transported to the Thermal Conductivity Laboratory to warm up. When necessary, holes were drilled in the core lining to relieve excess gas pressure. After thermal conductivity measurements were performed, each section was split along its orientation line by using two rotating saws mounted on a moving track. Both archive and working halves were scraped and cleaned. The archive half was used for description while the working half was subsampled. After sedimentological descriptions were recorded, the archive half was photographed and analyzed with a spectrophotometer. Both halves were then wrapped in thin plastic, packed in specially designed rectangular D-tubes, and stored in a refrigerated container. Additional details related to core handling are described in Winters and others (this volume, chapter 3).

Multi-Sensor Core Logger (MSCL)

Measurements of high-resolution sediment physical properties were obtained at 2-centimeter (cm) intervals by using a Geotek Multi-Sensor Core Logger (MSCL). These measurements comprise P-wave velocity, bulk density, and magnetic susceptibility. A summary description of the MSCL system is presented below, and a detailed description of the system and software can be found in the Geotek MSCL Manual (available in Appendix H). The MSCL consists of a conveyor system, a central unit assembly, a microprocessor, and a personal computer (PC). The conveyor system has a two-track section, mounted and aligned on either side of the central unit, and a belt-driven pusher block, which is driven in either direction by a stepper motor and gear box assembly. The central unit assembly incorporates a compressional wave (P-wave) logger, a gamma ray attenuation logger, and a magnetic susceptibility loop. A reference position is located 12 cm to the right of the P-wave logger. The gamma ray attenuation logger and magnetic susceptibility loop were offset to the left of a reference position 26 cm and 44 cm, respectively. The 1.5-m-long sections of split core were brought into the Geotek container and allowed to equilibrate to ambient temperature to reduce drift of the magnetic susceptibility measurements. The core section was then placed on the track to the right of the P-wave transducer, and the top of the core section was aligned with the reference zero position. A temperature probe was inserted in the core section to record core temperature. To ensure good acoustic coupling for the P-wave velocity measurements, the section liner was wiped down with a wet sponge, and distilled water was sprayed on the P-wave transducers. Each 1.5-m-long core section was placed on the right-hand track with the top located at the reference position and traveled incrementally past the P-wave logger, gamma ray attenuation logger, and through the magnetic susceptibility loop. After each increment of travel, a reading from each sensor was recorded. The MSCL measurements are presented in Appendix H (this volume).

Lithologic Description

Split sections were scraped to expose fresh sediment. Texture then was estimated through analysis of smear slides, tactile sensations, and taste. Grain-size results determined in a shore-based laboratory are presented in Winters and others (this volume, chapter 4). Textural components are described as clay (<2 micrometer (μm), silt (2–63 μm)), or sand (>63 μm).

Sediment textural names are:

- *Clay* (>80-percent clay);
- *Silt* (>80-percent silt);
- *Sand* (>80-percent sand);
- *Silty clay* (clay > silt; <80-percent silt or clay, <10-percent sand);
- *Clayey silt* (silt > clay; <80-percent clay or silt; <10-percent sand);
- *Sandy mud* (<80-percent silt or clay; 10- to 50-percent sand);
- *Muddy sand* (<80-percent silt or clay or sand; 50- to 80-percent sand).

Multimodal mixtures span a range of size classes. Both unimodal and multimodal sediment names and associated patterns are summarized in figure 3. Symbols for biogenic or genetically significant sediment components are displayed where this component exceeds 10 to 20 percent. In such cases, no vertical line separates the terrigenous textural symbol from the biogenic one. This implies that the components are intimately mixed in the sediment. Sediment with significant biogenic content has a name that indicates fossils are more abundant (for example, nannofossil silty clay). If the biogenic component exceeds 50 percent of the sediments, the sediment is called an ooze. Very thinly laminated sediments, with laminations too small to be differentiated, are indicated by using a split lithologic column with a vertical dividing line. Sedimentary structures, contacts, and grading are indicated by using the symbols in figure 3. Coring disturbances also are indicated by symbols in figure 3, and colors are designed using the Munsell classification. The sedimentological descriptions are presented in Appendix F.

Digital Photography

Digital core photographs, in 50-cm intervals, were taken with a Minolta/Agfa system (courtesy of Laboratoire des Sciences du Climat et de l'Environnement (LSCE), Gif-sur-Yvette, France). Adobe Photoshop and Actioncam were used to edit the photographs of the archive cores. If the working half of a core was photographed, a "W" suffix was placed after the section number of the saved file. The photos were saved in the highest quality JPEG format. Photographs of entire cores are presented in Appendix G. Individual photographs are available on CD by request to V. Bout-Roumazielles, (UMR 8110 CNRS, University of Lille I, 59655 Villeneuve d'Ascq, France) or email: Bout@univ-lille1.fr.

Spectrophotometry

A Minolta CM-2002 handheld spectrophotometer with an 8-millimeter (mm)-diameter optical sensor (courtesy of University of Aix-Marseille, France) was used to measure properties of the reflected light from split sediment cores. Spectral reflectance is measured in the frequency band near 40,000 nanometers (nm) and divided into 31 channels, each 10 nm in length. Reflectance was measured after the core was split, described, and photographed (an elapsed time of about 40 minutes). Measurements were made every 5 cm down the length of the core, wherever possible, and a white calibration was performed at the end of each section. The reflectance measurement also provides an estimate of the sediment color in the L*a*b Colour-Difference System and in Munsell notation. The estimation of the color should be used with care because the actual value is an average of an 8-mm-diameter section of sediment. The spectral reflectance in the longer wavelengths is useful in distinguishing layers of detrital carbonate (light color) that occurred in several cores. Color reflectance diagrams are presented in Appendix I.

Sedimentological Summary

The analysis of both sedimentological observations and spectral reflectance data provides preliminary interpretations on the dominant sedimentary processes occurring in each of the five geographical study areas: Tunica Mound, Bush Hill, Pigmy Basin, west of the Mississippi Canyon, and east of the Mississippi Canyon (Kane Spur) (fig. 2). The complete sedimentologic description of each core is contained in Appendix F, and a summary of the description is presented in this chapter and in Appendix E (this volume).

Tunica Mound

A number of cores were recovered in water depths of about 600 m adjacent to Tunica Mound along a 7-kilometer (km) transect (fig. 4). The principal cores that were sedimentologically described (from west to east) are labeled: MD02- 2545G, MD02-2537, MD02-2546, MD02-2535, MD02- 2541, MD02-2548, and MD02-2539. Visual and smear-slide observations indicate that the sediment mostly consists of silty clay and clay, and that the amount of foraminifers decreases with subbottom depth. Within cores MD02-2541 and MD02- 2539, a clear transition is observed in the upper few meters (0 to 4.5 meters below sea floor (mbsf) and 0 to 6 mbsf, respectively). This transition corresponds to a down core progressive decrease in the nannofossil and foraminifer content, and is reflected in a darkening color progression (fig. 5A, B).

Sedimentological Description Summary

MD02-2535 (37.84 m long)

Dominant lithologies:

0 to 9 mbsf: greenish gray to brown silty clay with nannofossils and in some intervals rich in foraminifera, bioturbated.

9 to 13.50 mbsf: layered dark gray silty clay, not bioturbated.

13.50 to 37.84 mbsf: brownish dark gray nannofossil clay with rare to common foraminifera, bioturbated.

Minor lithologies:

common organic-rich layers with black streaks, pyrite layers.

MD02-2537 (33.58 m long)

Dominant lithologies:

dark gray nannofossil clay with rare foraminifera.

18.7 to 23 mbsf: partially layered.

> 9 mbsf are disturbed by gas holes and voids.

Minor lithologies:

33.50 to 33.53 mbsf: ash layer.

MD02-2539 (31.10 m long)

Dominant lithologies:

0 to 6 mbsf: greenish gray to dark greenish gray sandy silt rich in foraminifera (upper 2 m) to greenish gray to dark greenish gray silty clay with foraminifera.

6 to 31.10 mbsf: dark gray clay, mostly contain faint layering; bioturbated.

Minor lithologies:

black organic-rich streaks are common.

MD02-2541 (35.34 m long)

Dominant lithologies:

0 to 4.5 mbsf: greenish gray to dark greenish gray silty clay with abundant foraminifera (upper 2.2 m) to greenish gray to dark greenish gray silty clay.

4.5 to 35.34 mbsf: dark gray clay with foraminifera, mostly contain faint layering; bioturbated.

Minor lithologies:

black organic-rich streaks common, several pyrite concretions.

MD02-2545G (9.27 m long)

Dominant lithologies:

greenish gray silty clay to dark gray clay with foraminifera, bioturbated, homogenous, gas voids common below 4.20 m, layered below 8.18 m.

Minor lithologies:

carbonate nodules, black streaks common.

MD02-2546 (31.21 m long)

Dominant lithologies:

0 to 21.00 mbsf: dark gray to greenish gray frequently layered clay with nannofossils and various amount of forams; bioturbation common to abundant.

10.50 to 18.00 mbsf: gas voids abundant

21.00 to 31.20 mbsf: greenish gray laminated silty clay with decreasing downward foram content, slightly bioturbated.

Minor lithologies:

Diagenetically modified sediments have formed some nodules (26.70 m) or are increasing the hardness of the sediment below 27.95 m.

MD02-2548 (32.93 m long)

Dominant lithologies:

0 to 18.00 mbsf: light greenish to greenish and brownish gray clay with some layers enriched in silt. Forams are present in some intervals. Layering occurs in most of this interval. Bioturbation is limited.

18.00 to 32.92 mbsf: greenish to dark greenish gray silty clay. Black streaks are common, slight bioturbation is present in most of the interval. Forams are not observed.

Minor lithologies:

28.28 to 28.30 mbsf: very light greenish gray ash layer with sharp contacts.

Preliminary Interpretations

Because the textural analyses were widely spaced within each core, they could not be used to compare different cores. However, the continuous spectrophotometer data (fig. 5A b) proved to be a useful proxy for carbonate content. However, chemical analyses are needed to

confirm this relation. Although the spectrophotometer data were useful, some problems were encountered. For example, the color reflectivity value displays systematically higher values along core MD02-2535 that could be due to poor calibration. The color of core MD02-2548 was not measured. The Holocene is clearly visible and displays a constant increase of color reflectivity from the last glacial with a noticeable drop in the middle of the curve, corresponding to the Younger Dryas cooling event (Broecker and others, 1988). Further interpretation is more difficult but seems to be possible between the eastern cores. Some high-frequency oscillations characterize the color reflectivity record before the last glacial maximum (fig. 5A, B). These oscillations mimic the stadials/interstadial oscillations of the last glacial cycle, the so-called Dansgaard/Oeschger oscillations (Johnsen and others, 1992; Bond and others, 1993; Dansgaard and others, 1993). Lower values of the color reflectivity characterizing the lower part of core MD02- 2535 (below 23.00 m) may correspond to the Marine Isotopic Stage 4 (fig. 5A). Using only this approach, it seems the sedimentation rate increases to the east.

Tunica Mound Special Features

The seven cores sampled in the Tunica Mound area display special features that do not correlate well with depth or age:

- Diagenetic nodules occur in core MD02-2537 within the interval 30.57 to 30.70 mbsf. However, the nodules appear in core MD02-2546 near 26.70 mbsf.
- Hardness increases below 27.95 mbsf in core MD02-2546.
- Some core intervals display iron (?) sulfide traces, most often in the lower sections. For example, core MD02-2537 at about 27.00 m, core MD02-2541 below 28.00 m, and in the lower end of core MD02-2539. Even if pyrite is not observed, the presence of iron sulfide may be responsible for the black streaks in cores MD02- 2535, MD02-2539, MD02-2541, MD02- 2545G, and MD02-2548. These intervals may be enriched in organic matter.
- Some cores display voids that may have been caused by the escape of gas.

Bush Hill

Four cores were collected at Bush Hill along a 2.2- km-long profile in water depths ranging from 602 to 654 m (fig. 6). Visual and smear-slide observations indicate that the upper sediment (to a depth of 8.0 mbsf) mostly consists of clay and silty clay containing

foraminifera. The upper part of cores MD02-2554 and MD02-2555 display similar color trends with decreasing color reflectivity (related to decreasing foraminifer content) down core, followed by increasing reflectivity (fig. 7).

Sedimentological Description Summary

MD02-2554 (31.05 m long)

Dominant lithologies:

0 to 6.00 mbsf: greenish to dark greenish gray silty clay with coccoliths and foraminifers. Bioturbation slight, black streaks common along some intervals.

6.00 to 12.00 mbsf: dark greenish to brownish clay without visible foraminifer.

12.00 to 31.05 mbsf: laminated dark greenish gray clay with little bioturbation.

Numerous voids caused by gas expansion and gas pockets. Rare to absent foraminifers.

Minor lithologies: None.

MD02-2555 (35.68 m long)

Dominant lithologies:

0 to 9.00 mbsf: greenish gray bioturbated clay with common foraminifers.

9.00 to 35.68 mbsf: light to dark greenish gray layered clay with bioturbation.

Minor lithologies:

19.63 to 19.65 mbsf and 21.60 to 21.63 mbsf: silty, organic-rich layers.

MD02-2556 (34.25 m long)

Dominant lithologies:

dark greenish to dark brownish gray clay with some foraminifers. Gas pockets are present throughout the core.

Preliminary Interpretations

The color reflectivity records (fig. 7) provide good correlations among the cores of the Bush Hill area (fig. 6). The Holocene is clearly characterized on all cores by the highest values of the color reflectivity. These high values may correspond to an increased carbonate content of the sediment deposited during the Holocene. A darker interval in the color reflectivity record near 4.50 mbsf in cores MD02-2554 and MD02-2555 (fig. 7) and around 2.50 mbsf in core MD02-2557GHF (fig. 7) could correspond to the cold Younger Dryas event (Broecker and others, 1988). The last glacial maximum (LGM) may be marked by the

lowest values (between 5.00 mbsf and 6.00 mbsf in cores MD02-2554 and MD02-2555) of the color reflectivity (that is, the lowest carbonate content and highest detrital content), reflecting the general decrease of the primary productivity in the Gulf of Mexico during this period. Correlations are less evident between cores MD02- 2554/55 and core MD02-2557GHF.

Bush Hill Special Features

- The lower half of core MD02-2554 contains numerous voids caused by gas expansion. These voids are only observed in laminated to faint layered clay, usually without foraminifera. These voids are not observed in cores MD02-2555 or MD02- 2556 (except along a few intervals), but sulfide traces or black organic-rich lenses are observed at similar depths.
- Pyrite cubes or dispersed iron (?) sulphides as black spots or streaks are more common in the lower half of the cores.

Pigmy Basin

One giant square box core (CASQ; C2 or C2) (MD02- 2553C2) was sampled in Pigmy Basin (figs. 2, 8). The sediment consists of sandy to silty clay with foraminifers and coccoliths to 1.55-m subbottom depth. The rest of the core (1.55 to 10.32 mbsf) consists of bioturbated clay with foraminifers.

Sedimentological Descriptions Summary

MD02- 2553C2 (10.03 m long)

Dominant lithologies:

0 to 1.55 mbsf: sandy to silty clay with foraminifers and coccoliths.

1.55 to 10.32 mbsf: greenish to dark greenish gray bioturbated clay with foraminifers.

Minor lithologies and special features:

0.58 to 0.60 mbsf, 3.00 to 3.02 mbsf, 4.00 to 4.02 mbsf, 4.20 to 4.22 mbsf, 5.81 to 5.95 mbsf, and 9.70 to 9.81 mbsf: foraminifer-rich intervals interpreted as turbidites, some with clearly defined upward fining texture.

Mississippi Canyon and Kane Spur

A series of piston and giant square box (CASQ; C2 or C2) cores were obtained in the Mississippi Canyon area in three distinct sub-areas (fig. 9). Note that cores MD02-2565 and MD02-2569 were not opened onboard.

Sedimentological Description Summary

MD02-2559 (33.39 m long)

Dominant lithologies:

0 to 3.50 mbsf: light to dark greenish grey bioturbated silty clay with some foraminifers.
3.50 to 28.80 mbsf: laminated, then layered light to dark greenish gray silty clay with few bioturbated intervals and no foraminifer visible. Below 8.33 mbsf: sand or silts layers or pockets throughout the core.

Minor lithologies:

thin layers and pockets of sand and silt.

MD02-2561 (28.8 m long)

Dominant lithologies:

0 to 4.50 mbsf: light to dark greenish gray silty clay with moderate bioturbation and some foraminifers with decreasing content down core.
4.50 to 9.00 mbsf: dark greenish gray laminated silty clay. No foraminifer visible.
9.00 to 28.80 mbsf: clay, then silty clay, slightly bioturbated.

Minor lithologies:

Numerous silt layers at the bottom of the core, for example, at 14.30 mbsf.

MD02-2562 (26.09 m long)

Dominant lithologies:

greenish to light greenish gray layered silty clay. Some bioturbation. Rare to absent foraminifers. Some layers are composed of upward fining silty clay.

Minor lithologies: None.

MD02-2563C2 (3.86 m long)

Dominant lithologies:

light to dark greenish gray with common tar (bitumen) spots and sandy layers. Forams are rare except in the upper part of the core.

Minor lithologies: None.

MD02-2566 (26.05 m long)

Dominant lithologies:

light to dark greenish gray silty clay with some layering. Foraminifers visible in the upper 2.60 m of the core with coccoliths. Silt layers occur from 14.00 mbsf to the bottom of the core.

Minor lithologies: None.

MD02-2567 (26.65 m long)

Dominant lithologies:

0 to 13.15 mbsf: greenish gray clay with subtle laminations. Foraminifers abundant to 3.85 mbsf.

13.15 to 26.65 mbsf: layered greenish gray silty clay. Increase of bioturbation. below 18.50 mbsf: increased bioturbation. Silty layers at several depths including 10.74 m.

Minor lithologies: None.

MD02-2570 (28.50 m long)

Dominant lithologies:

0 to 6.50 mbsf: greenish to dark greenish gray silty clay with strong H₂S smell below 1.50 mbsf.

6.50 to 18.00 mbsf: dark greenish gray to dark gray silty clay with numerous gas bubbles or voids.

18.00 to 21.00 mbsf: clay. below 24.00 mbsf: greenish to light greenish gray silty clay with gas bubbles and voids. Some organic-rich layers and spots. Most of the core is slightly bioturbated.

Minor lithologies: None.

Preliminary Interpretations

Only the Kane Spur cores and one from the west Mississippi Canyon area were split. Therefore, only these cores will be sedimentologically described. In every core, visual and smear-slide observations indicate that the sediment mainly consists of dark greenish silty clay with a common two-fold system: an upper interval with some foraminifers and a lower interval with rare to absent foraminifers. The transition depth varies from core to core. In

some cores, the lowermost section of the core consists of coarser material containing sand and silt layers. The color reflectivity records of the Kane Spur cores are used for correlation purposes (fig. 10A, B). The upper part (0 to 3.00 mbsf) of cores MD02-2558, MD02-2560, MD02-2561, MD02-2562, MD02-2564GHF, MD02-2566, and MD02-2568GHF is characterized by high color reflectivity related to a high carbonate content, which was observed in the smear slides. This interval is believed to be Holocene in age. The Younger Dryas cold event (Broecker and others, 1988) is also tentatively identified in most of the cores by slightly lower values of color reflectivity when compared to Holocene sediments (less carbonate content and increased detrital content). The last glacial maximum is characterized by a decrease of the carbonate content as shown by the color reflectivity. Drastic cold climatic conditions prevented the development of primary nannofossil production during that time. Some high frequency oscillations characterize the color reflectivity record before the last glacial maximum (fig. 10A, B). These oscillations mimic the stadials/interstadial oscillations of the last glacial cycle, the so-called Dansgaard/Oeschger oscillations (Johnsen and others, 1992; Bond and others, 1993; Dansgaard and others, 1993).

References

- Balsam, W.L., and Beeson, J.P., 2003, Sea-floor sediment distribution in the Gulf of Mexico: Deep-Sea Research I, v. 50, p. 1421–1444.
- Bond, G., Broecker, W., Johnsen, S.J., McManus, J., Labeyrie, L., Jouzel, J., and Bonami, G., 1993, Correlations between climate records from North Atlantic sediments and Greenland ice: Nature, v. 365, p. 143–147.
- Bouma, A.H., Normark, W.R., and Barnes, N.E., eds., 1985, Submarine fans and related turbidite systems: New York, Springer, 351 p.
- Broecker, W.S., Andree, M., Wolfli, W., Oeschger, H., Bonami, G., Kennett, J., and Peteet, D., 1988, The chronology of the last deglaciation—implications to the cause of the Younger Dryas event: Paleoceanography, v. 3, no. 1, p. 1–19.
- Burk, C.A., and Drake, C.L., eds., 1974, The geology of continental margins: Berlin, Springer-Verlag.
- Coleman, J.M., Roberts, H.H., and Bryant, W.R., 1991, Late Quaternary sedimentation, *in* Salvador, A., ed., The Gulf of Mexico basin: Geological Society of America, p. 325–352.
- Cooper, A.K., and Hart, P.E., 2002, High-resolution seismic reflection investigation of the northern Gulf of Mexico gas-hydrate-stability zone: Marine and Petroleum Geology, v. 19, no. 10, p. 1275–1293.

- Dansgaard, W., Johnsen, S.J., Clausen, H.B., Dahl-Jensen, D., Gundestrup, N.S., Hammer, C.U., Hvidberg, C.S., Steffensen, J.P., Sveinbjörnsdóttir, A.E., Jouzel, J., and Bond, G., 1993, Evidence for general instability of climate from a 250-kyr ice-core record: *Nature*, v. 364, p. 218–220.
- Davies, D.K., and Moore, W.R., 1970, Dispersal of Mississippi sediment in the Gulf of Mexico: *Journal of Sedimentary Petrology*, v. 40, p. 339–353.
- Griffen, G.M., 1962, Regional clay-mineral facies-product of weathering intensity and current distribution in the northeastern Gulf of Mexico: *Geological Society of America Bulletin*, v. 73, p. 737–768.
- Johnsen, S.J., Clausen, H.B., Dansgaard, W., Fuhrer, K., Gundestrup, N.S., Hammer, C.U., Kersen, P., Jouzel, J., Stauffer, B., and Steffensen, J.P., 1992, Irregular glacial interstadials recorded in a new Greenland ice core: *Nature*, v. 359, p. 311–313.
- Mazzullo, J., 1986, Sources and provinces of late Quaternary sand on the East Texas-Louisiana continental shelf: *Geological Society of America Bulletin*, v. 97, p. 638–647.
- Mazzullo, J., and Bates, C., 1985, Source of sand for the northeast Gulf of Mexico shelf and the Mississippi fan: *Gulf Coast Association of Geological Societies Transactions*, v. 35, p. 457–466.
- Nairn, A.E.M., and Stehli, F.G., 1975, *The Gulf of Mexico and the Caribbean: The Ocean Basins and Margins*, 3, New York, Plenum Press, 706 p.
- Sassen, R., Sweet, S.T., Milkov, A.V., DeFreitas, D.A., Salata, G.G., and McDade, E.C., 1999, Geology and geochemistry of gas hydrates, central Gulf of Mexico continental slope: *Gulf Coast Association of Geological Societies Transactions*, v. 49, p. 462–468.

Figure Captions

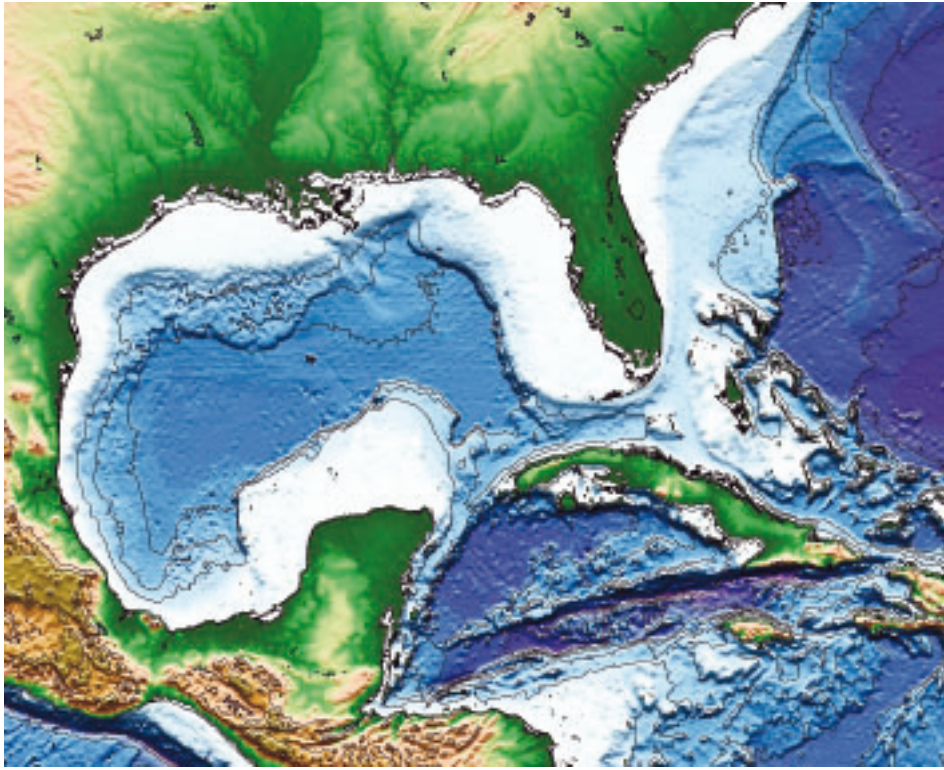


Figure 1. Bathymetry and morphology of the Gulf of Mexico.

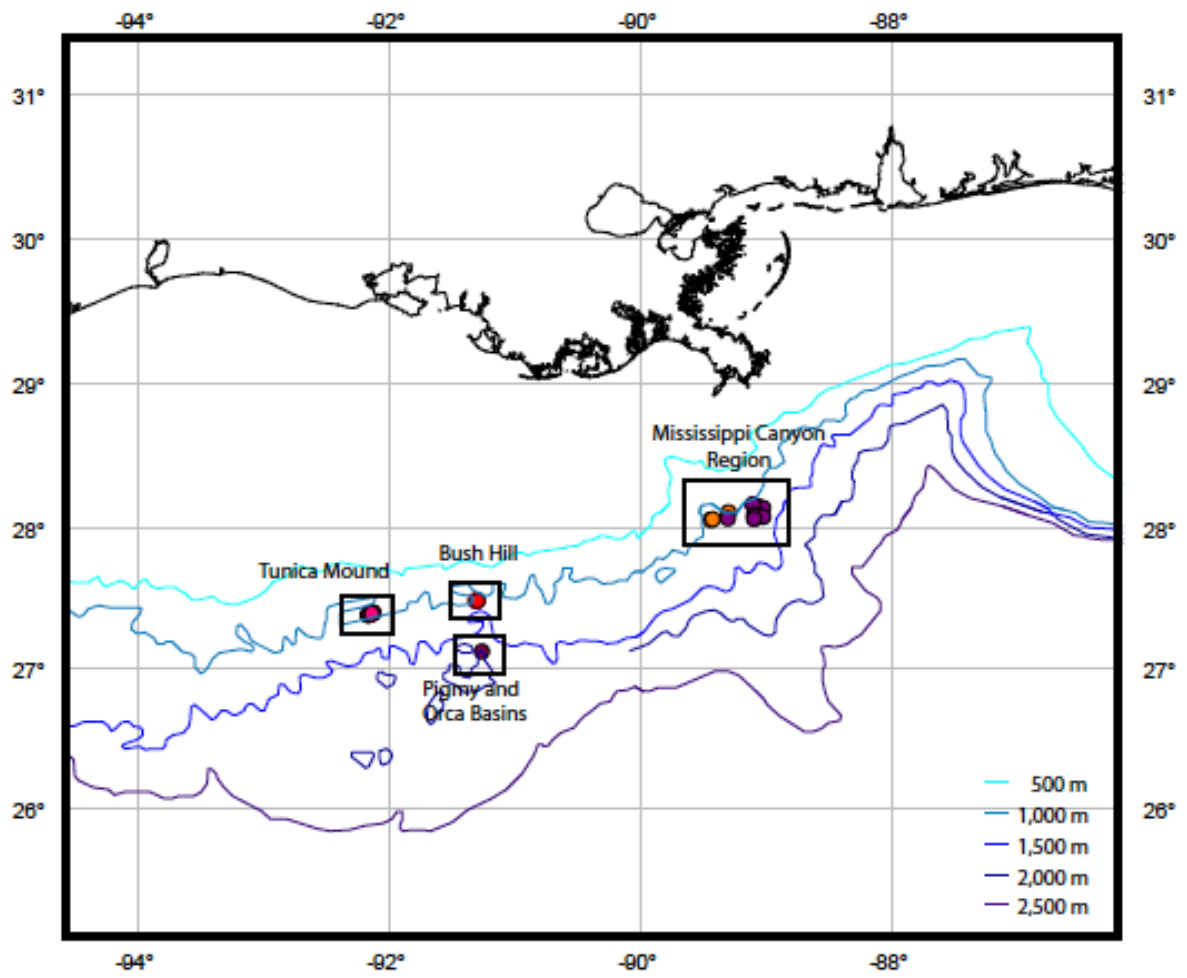
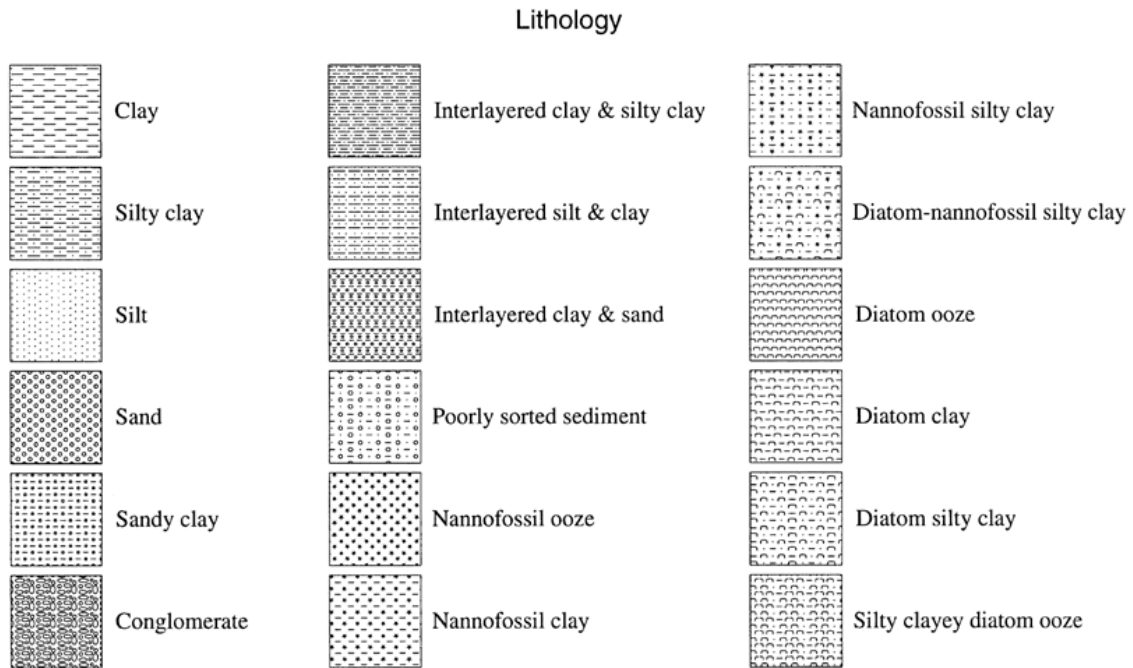


Figure 2. General map of the IMAGES VIII/PAGE 127 cruise.

Legend for Core Description



Structure and Drilling Disturbance

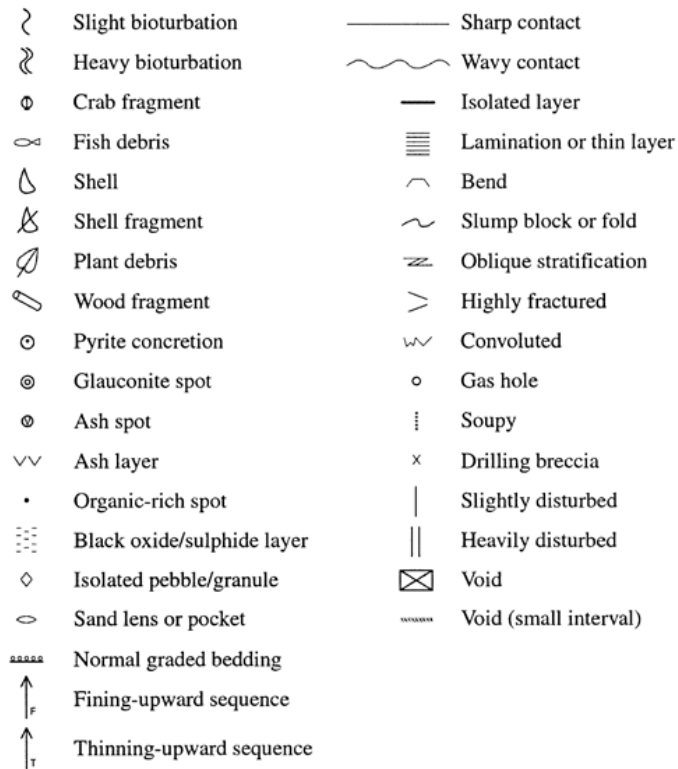


Figure 3. Legend for core descriptions.

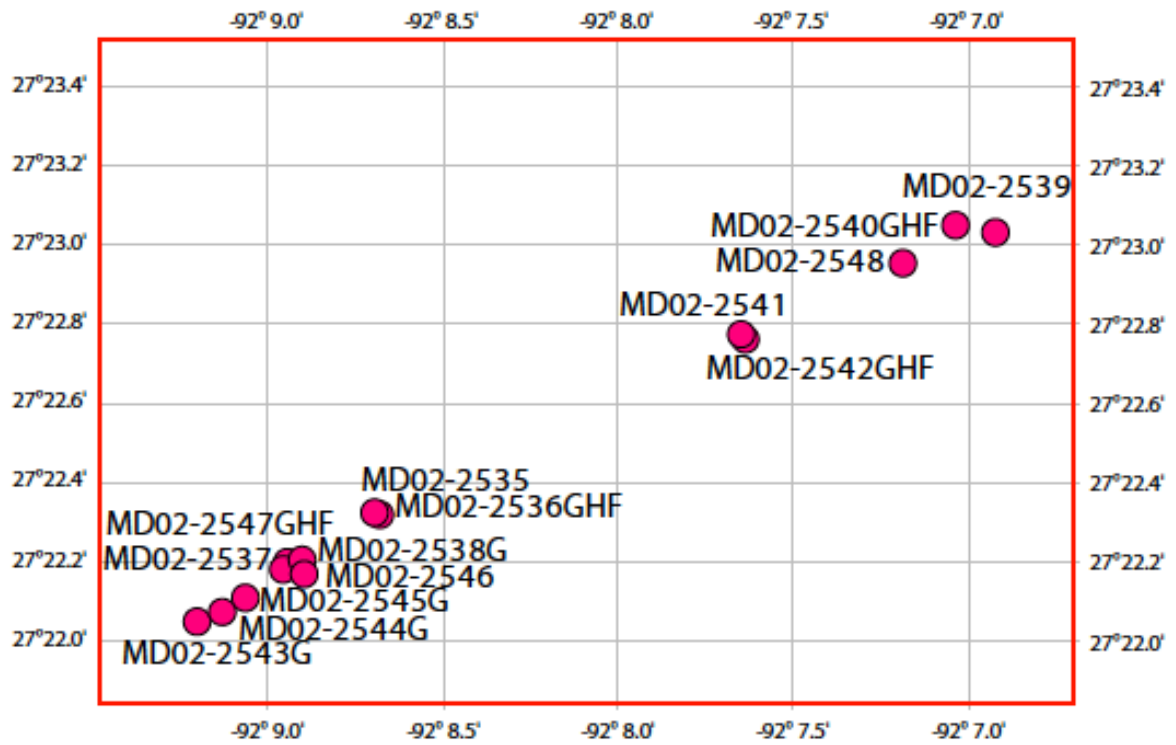


Figure 4. Tunica Mound core locations.

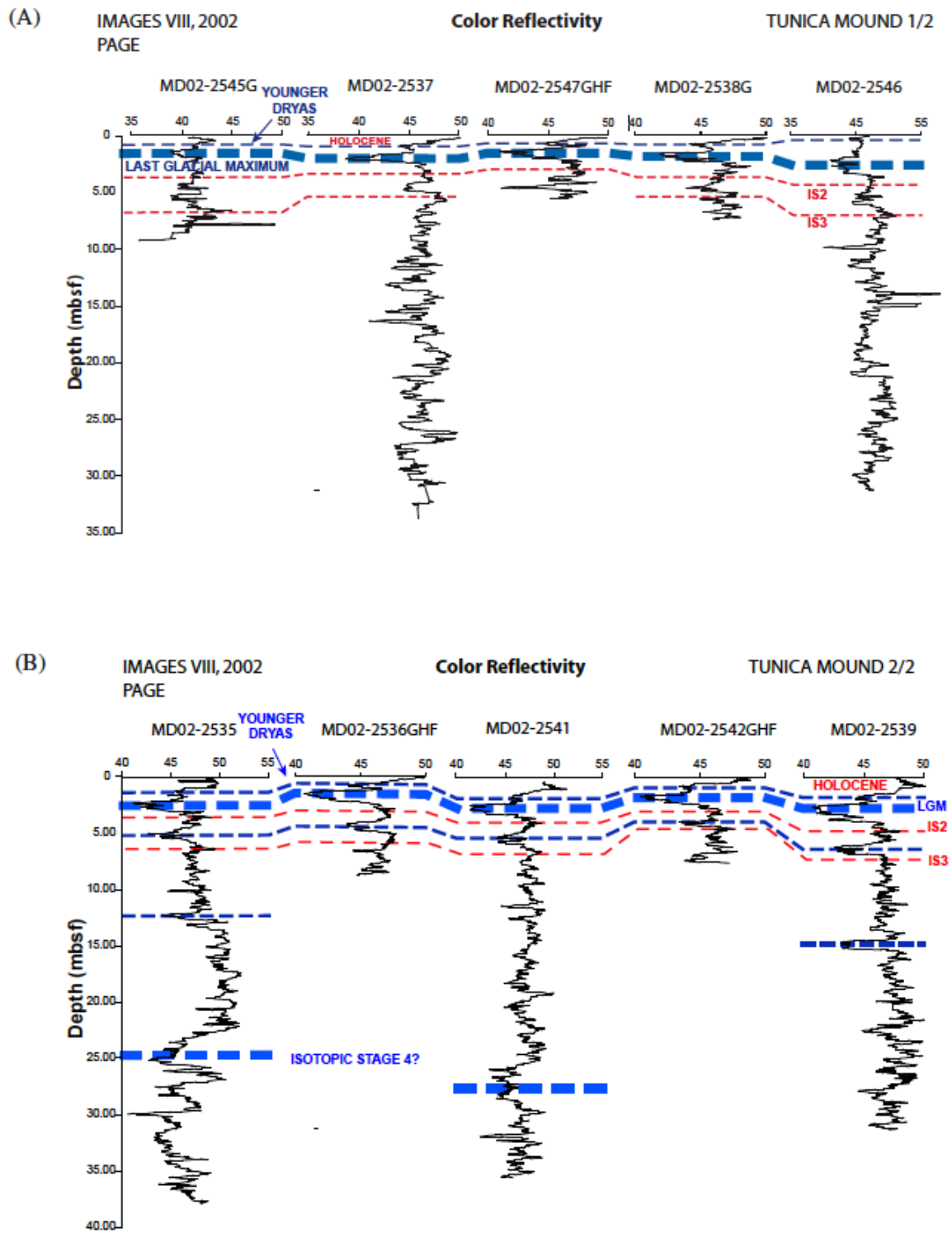


Figure 5. Color reflectivity for (A) cores located in the southwestern Tunica Mound study area and (B) cores located in the northeastern Tunica Mound study area.

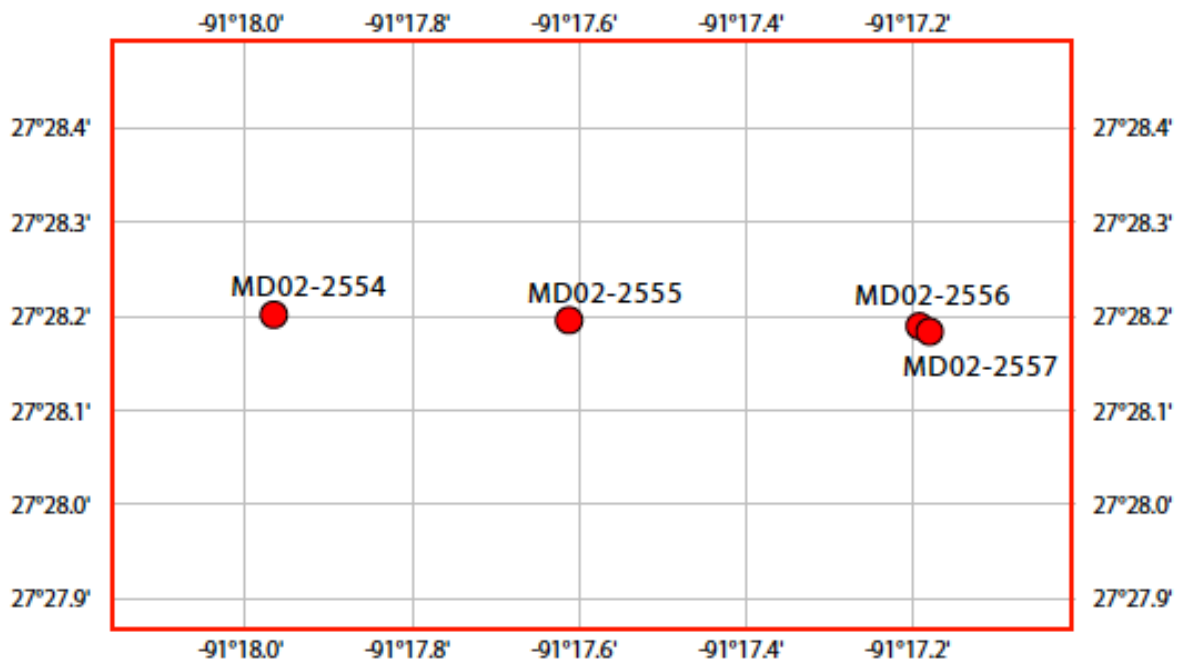


Figure 6. Bush Hill core locations.

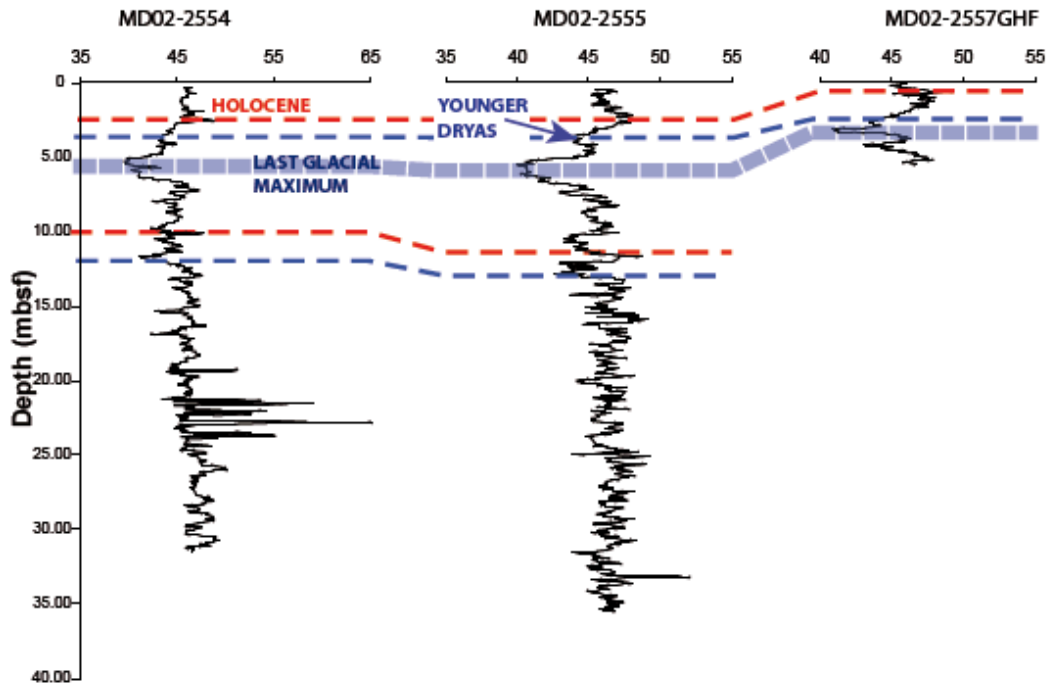


Figure 7. Color reflectivity for Bush Hill cores MD02-2554 to MD02-2557GHF.

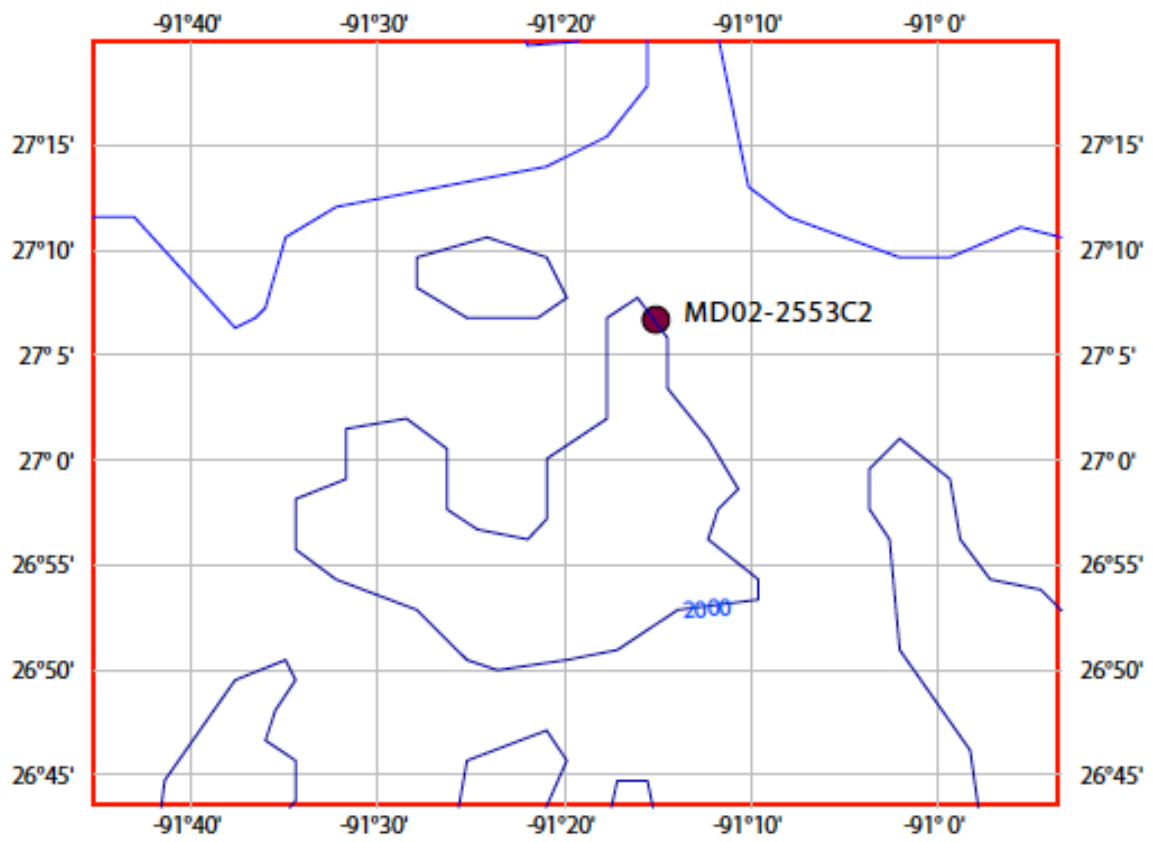


Figure 8. Location of Pigmy Basin core MD02-2553C2.

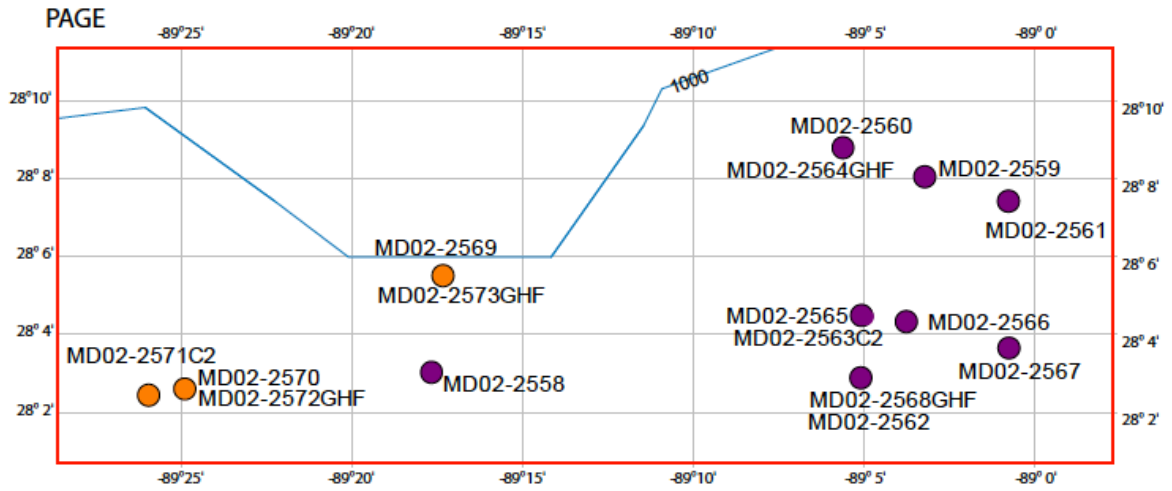


Figure 9. Core sites west of the Mississippi Canyon (MD02-2570, -2571C2, and -2572GHF), in the Mississippi Canyon (MD02-2558 (not a USGS core), -2569, -2573GHF), and east of the Mississippi Canyon (Kane Spur) (MD02-2559 to -2568GHF).

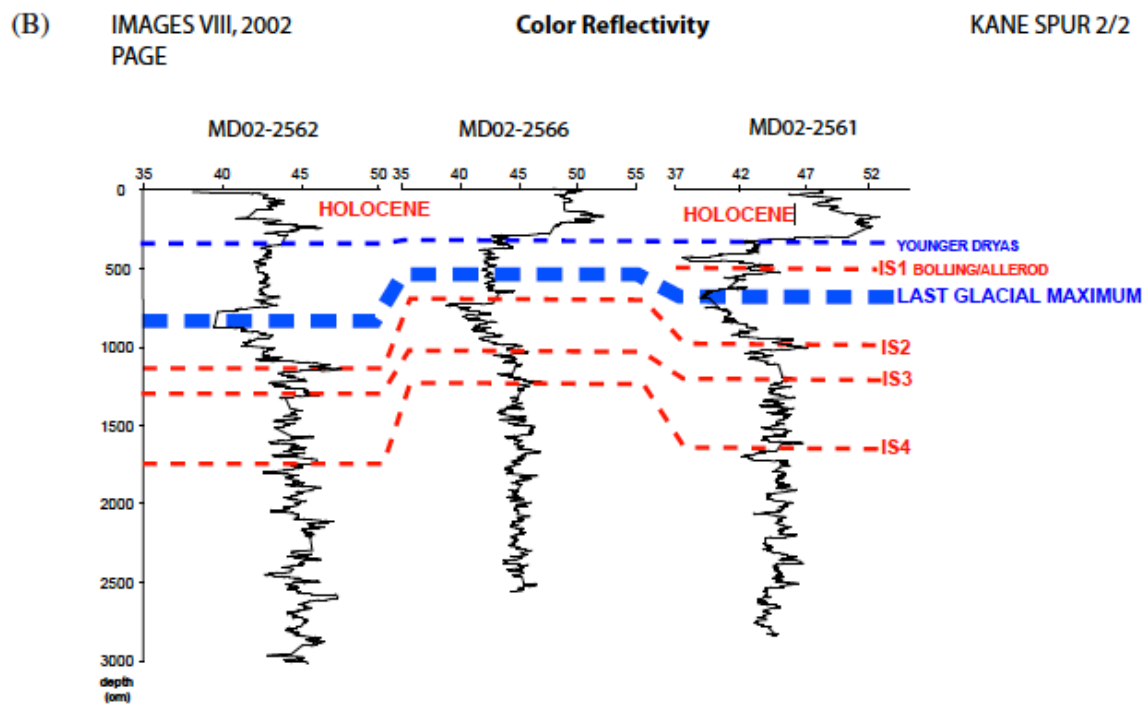
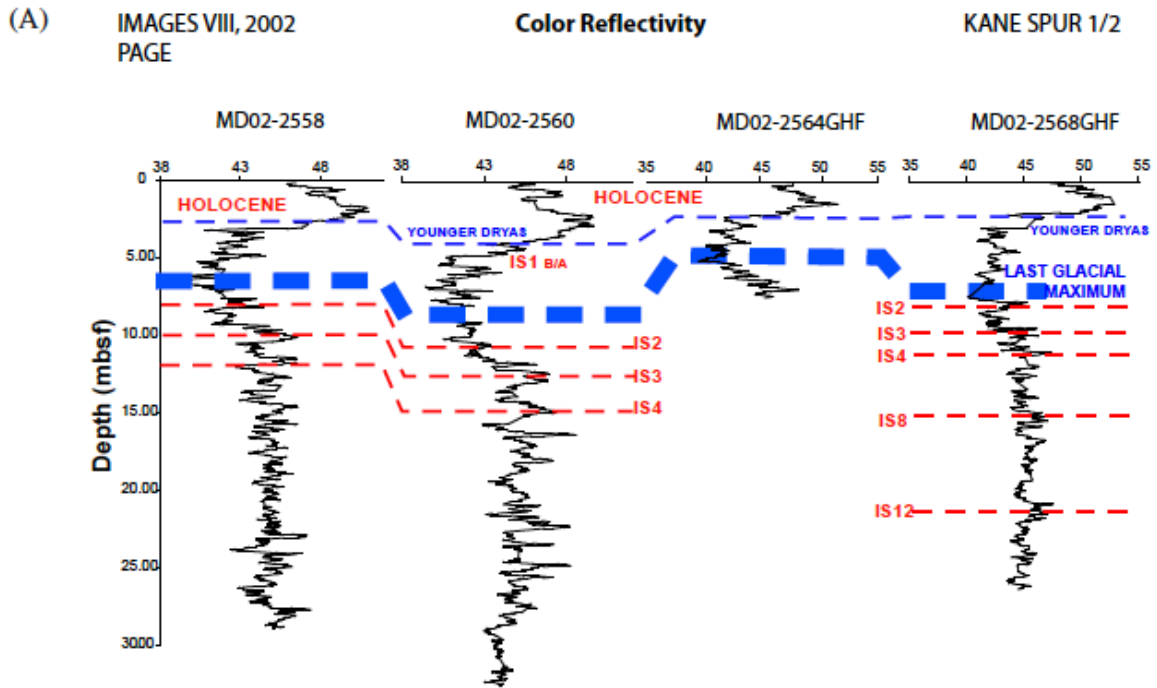


Figure 10. Color reflectivity for (A) Mississippi Canyon cores MD02-2558 (not a USGS core) to MD02-2568GHF and (B) Mississippi Canyon (Kane Spur) cores MD02-2562 to MD02-2561.